Hindawi
International Journal of Polymer Science
Volume 2019, Article ID 1412737, 8 pages
https://doi.org/10.1155/2019/1412737

Research Article

Controlled Release of Ropivacaine from Single-Armed (1-PCL) and Four-Armed PCL (4-PCL) Microspheres

Wei Xiong,[1] Yue-kun Shen,[1] Peng Dong,[2] Ying Xiao,[1] Xiong-qing Huang,[1] Wen-qi Huang,[1] Lu Yang,[1] and Xia Feng[1]

[1]*Department of Anesthesiology, The First Affiliated Hospital of Sun Yat-sen University, 510080 Guangzhou, Guangdong Province, China*
[2]*State Key Laboratory of Applied Microbiology Southern China, Guangdong Provincial Key Laboratory of Microbial Culture Collection and Application, Guangdong Institute of Microbiology, 510070 Guangzhou, China*

Correspondence should be addressed to Lu Yang; sumsyanglu@163.com and Xia Feng; fengxiar@aliyun.com

Received 28 March 2019; Revised 21 May 2019; Accepted 5 June 2019; Published 3 July 2019

Academic Editor: Mehdi Salami-Kalajahi

Sustained release of anesthesia has shown great promise in the treatment of chronic pain in patients. In this research, we used neutralized ropivacaine as an anesthesia and poly(ε-caprolactone) (PCL) with different architectures to systematically study how these architectures affect the release of ropivacaine. After optimizing the parameters of the preparation of microspheres, ropivacaine-loaded 1-PCL microspheres and 4-PCL microspheres were obtained. Fourier Transform infrared spectra (FT-IR) and X-ray diffraction spectra (XRD) confirmed that ropivacaine was encapsulated within the microsphere rather than inserted on the surface of the microsphere. Ropivacaine was found to be buried deeper in the 1-PCL microsphere than in the 4-PCL microsphere. *In vitro* release assay revealed that small crystalline grains interfered with ropivacaine release in 4-PCL microspheres during the initial release period, but then two kinds of microspheres showed a similar ropivacaine release rate. We basically proved that the architecture of PCL has a negligible effect on ropivacaine release. Cell proliferation test revealed that the release of products from the microspheres resulted in insignificant toxicity towards mammalian cells.

1. Introduction

Ropivacaine is a long-term local amide anesthetic with low toxicity towards both the central nervous system and the cardiovascular system [1, 2]. In particular, ropivacaine can separately block the sensory and motor nerves, which is beneficial to the management of intractable pain that occurs during such as trigeminal neuralgia and advanced cancer [3–5]. The duration of current ropivacaine formulation is almost shorter than 12 hours [6, 7]. Intermittent injection of ropivacaine has to be applied to alleviate chronic pain. But the risks of indwelling catheter blockage and infection have a huge additional burden on patients under chronic pain [8, 9].

Microsphere-formulated drugs can prolong the duration of the drug and reduce administration frequency by controlling the release behavior [10–12]. The microsphere formulation can also help establish the medication compliance of the patients [13]. Several studies on the microsphere-formulated ropivacaine have shown promise in the controlled release of drugs. Chitosan microspheres loaded with ropivacaine hydrochloride show linear release [14]. Ropivacaine hydrochloride carried by poly(lactic-*co*-glycolic acid) (PLGA) has been found to prolong the release period during animal experiments [15]. Polyethylene glycol monostearate, medium-chain triglyceride, and lipoid have been used to fabricate nanocapsules for transdermal ropivacaine delivery with fine efficiency [16]. However, the immunogenicity of gelatin, strong acidity of degradation products of PLGA, and relatively high cost of lipid carriers might limit the application of ropivacaine microspheres.

PCL is a biocompatible polyester with a long degradation period [17–19]. Moreover, the degradation products of PCL have relatively high pK_a which prevents noninflammatory

reactions [20]. In this work, PCL-loaded ropivacaine microspheres (Ropi-PCL particles) were prepared through the O/W method using single-armed PCL (1-PCL) and 4-armed PCL (4-PCL) as carrier materials. We systematically studied the parameters which affected microsphere morphology and their release behavior. Furthermore, we used the optimized preparation conditions to fabricate PCL particles that could load ropivacaine. Release kinetics of the ropivacaine-loaded PCL microspheres were studied, and the released products did not exert significant toxicity on mammalian cells. This research sets the foundation for the *in vivo* application of ropivacaine-loaded PCL microspheres in nerve blockage experiments.

2. Materials and Methods

2.1. Materials. Ropivacaine hydrochloride injection (Naropin®, 100 mg/10 mL, AstraZeneca) was used. Stannous octoate ($Sn(Oct)_2$), polyvinyl alcohol (1797, alcoholysis degree 96.0-98.0%), dichloromethane (DCM), toluene, and caprolactone (ε-CL) were purchased from Aladdin Biochemical Technology Co. Ltd. ε-CL was dried over CaH_2 and distilled under reduced pressure before use. All the other solvents were dried by CaH_2 before use.

2.2. Characterization. ^1H (300 MHz) and ^{13}C NMR (75 MHz) spectra were recorded by a Mercury-Plus 300 spectrometer (Varian Inc., America) using $CDCl_3$ as solvents with 0.5% tetramethylsilane as the internal standard. Gel permeation chromatography (GPC) measurements were performed on a Waters 1525 binary high-pressure liquid chromatography (HPLC) pump equipped with 3 Ultrastyragel columns and a Waters 2414 refractive index detector (Waters Alliance GPC 2000, Waters Corporation, America). THF was used as the eluent at a flow rate of 1 mL/min at 40°C. GPC samples were prepared with a concentration of 1 mg/mL.

The thermal properties of the polymers were determined by differential scanning calorimeter (DSC) (TA Instruments Q10) with a heating rate of 10°C/min.

A scanning electron microscope (SEM) (HITACHI, H-3000N) was utilized to characterize the morphology of blank and degraded polymeric microspheres.

Mastersizer 2000 (Malvern Instrument Ltd. Co., Worcestershire, UK) was used to determine the size and size distribution of polymeric microspheres. The results are presented as the average values of five measurements.

The UV spectra were recorded by a Lambda 45 UV-VIS spectrophotometer (PerkinElmer).

The FT-IR spectra were recorded by a TENSOR II (Bruker).

2.3. Synthesis of Carrier 1-PCL and 4-PCL. PCL was synthesized according to a modified method as reported by Qiang et al. [21]. Briefly, benzyl alcohol (BnOH) and pentaerythritol were separately used as initiators to polymerize ε-CL under the catalysis of $Sn(Oct)_2$ at 110°C. After polymerization for 24 h, the vials were cooled to room temperature. Products were dissolved in DCM and precipitated by cold methanol. The process was carried out twice. The obtained polymers were dried under vacuum for 48 h.

2.4. Neutralization of Ropivacaine Hydrochloride. Pure ropivacaine was prepared by neutralizing Naropin®. The ropivacaine hydrochloride injection solution was placed in a beaker, and 10 eq. of aqueous ammonia was added dropwise into the beaker. A water-insoluble white precipitate formed immediately. The precipitate was collected by filtration and washed by deionized water until the pH turned to 7. The filter mass was dried in a vacuum to obtain constant weight.

2.5. Preparation of Ropivacaine-Loaded PCL Microsphere. The microspheres were prepared via a single emulsion method (O/W). The effect of the PCL dosage, ropivacaine dosage, PVA dosage, and O/W ratio was separately investigated. Then, the optimized microspheres were fabricated. Both drug loading (DL) and encapsulation efficiency (EE) were assessed by the UV-vis method. DL and EE were assessed by the following equations:

$$\begin{aligned} \mathrm{DL} &= \frac{\text{Drug in microparticles}}{\text{Weight of microparticles}} \times 100\%, \\ \mathrm{EE} &= \frac{\text{Capsulated drug}}{\text{Total drug}} \times 100\%. \end{aligned} \tag{1}$$

2.6. In Vitro Release of Microspheres. Precisely weighted optimized particles were placed in dialysis bags (MWCO = 1000 kDa), and the fastened dialysis bags were completely immersed in 35.0 mL phosphate-buffered saline (PBS, pH = 7.4). They were then incubated in a shaker incubator at 50 rpm at 37 ± 1°C. After, 5 mL of the PBS samples was obtained and an equal volume of fresh PBS was added at 1, 2, 4, 8, 28, and 58 h ($n = 3$). The samples were analyzed by the UV-vis method.

2.7. Cytotoxicity Test. Mouse fibroblast L929 cells were kindly provided by Prof. Quan's group. The cells were cultured in DMEM medium, which contained 10% fetal bovine serum (FBS) and 1% penicillin/streptomycin solution. The cells were incubated in culture bottles at 37°C and 5% CO_2 (BPN-50CH, Yiheng, China). The culture medium was changed every 2 days. Cells at passage three were used in the experiments.

Cell cytotoxicity was evaluated by the Cell Counting Kit-8 (CCK-8; meilunbio) according to the manufacturer's instructions. L929 were seeded in the 96-well plate at a density of 3000 cells/well and cultured for 4 h. Then, 10 μL sterilized microsphere release sample was added to the wells and cultured overnight. Finally, the culture media were removed, and the cells were washed by PBS for 3 times. DMEM with 10% CCK-8 was added to each well. After a 2 h incubation, the 96-well plate was transferred in order to read the optical density (OD) value at 450 nm.

Table 1: Ring-opening polymerization of ε-CL catalyzed by $Sn(Oct)_2$.

Entry[a]	Initiator	[*I*]/[*M*]	DP[b]	Mn (kDa)[c]	Mn (kDa)[d]	PDI[d]	Tg (°C)[e]	Tm (°C)[e]
1-PCL	Benzyl alcohol	1/100	106	12.2	8.3	1.39	-56.8	54.4
4-PCL	Pentaerythritol	1/100	27.5	12.6	13.7	1.34	-57.7	52.7

[a]Bulk polymerization was conducted at 110°C for 24 h. The polymerization applied $Sn(Oct)_2$ as the catalyst. [b]Methylene of benzyl alcohol served as a reference to calculate DP of 1-PCL: $DP_{1-PCL} = I_{(4.06ppm)}/2$; methylene of the terminal group CH_2OH served as a reference to calculate DP of 4-PCL: $DP_{4-PCL} = (I_{(4.06ppm)}/2)/4$. [c]Mn was determined by ^1H NMR and the deuterium solvent was $CDCl_3$. [d]Mn and PDI were determined by GPC using polystyrene as calibration. THF was in the mobile phase. [e]Thermal analysis was measured by DSC with a heating rate of 10°C/min under N_2 flow.

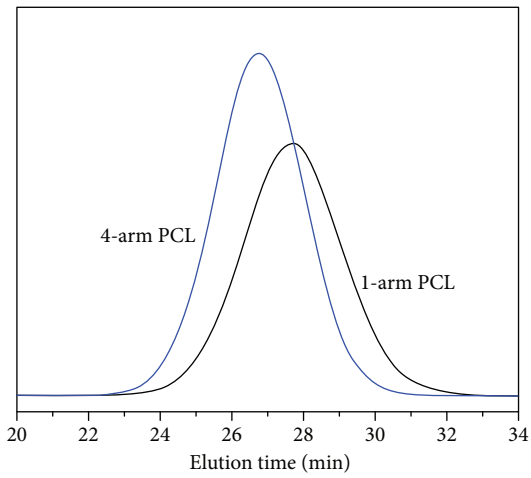

Figure 1: GPC curves of 4-arm PCL (blue) and 1-PCL (black).

3. Results and Discussion

3.1. Synthesis of 1-PCL and 4-PCL. PCL is a biocompatible semicrystalline polyester and is widely applied as a scaffold in tissue engineering for controlled release. There have been few reports on PCL serving as a carrier of ropivacaine [22]. In this work, we focused on the effect of PCL structure towards loading and release of ropivacaine.

We applied $Sn(Oct)_2$ as the catalyst to synthesize single- and four-armed PCLs. As indicated in Table 1, the degree of polymerization (DP) of PCL coincided with the feed ratio of the initiator and ε-CL monomer. It showed that $Sn(Oct)_2$ can effectively control the structure of PCL by ring-opening polymerization (ROP), which is beneficial in serving as a carrier. The hydrodynamic radius of 4-PCL is different from 1-PCL and is responsible for the change in Mn as determined by GPC (Figure 1).

3.2. Neutralization of Ropivacaine Hydrochloride. Since ropivacaine hydrochloride is highly soluble in DI water, it hinders the loading efficiency of PCL. We neutralized Naropin® with aqueous ammonia. White precipitation formed immediately when aqua ammonia was added. Excess ammonia was washed off by DI water until the pH became neutral. Pure ropivacaine (Ropi) was obtained by lyophilization.

Comparing the ^1H NMR spectra of Naropin® and Ropi, we found that peaks shifted after neutralization. This originated from the interaction between deuterium solvent and the molecules. Further NMR data analysis confirmed that the structure and chirality is unchanged after neutralization since the integration of the characteristic peak is present (Figure 2). Hence, neutralization reaction just removes the hydrochloride and there is no change in the ropivacaine backbone. This indicates that the neutralized Ropi does not change the analgesia mechanism.

We used the UV-vis spectra to quantify ropivacaine. Ropi formed a peak absorbance at 229 nm (Figure S1A). The absorbance was used to set up a standard working curve in DCM and PBS. Both working curves showed a good linear relationship between the concentration of Ropi and absorbance (Figures S1B and S1C).

3.3. Preparation of Ropi Microspheres and Characterization. Ropivacaine has a good effect on analgesia and exhibits low toxicity towards the neutral system. It is hypothesized that the encapsulation of ropivacaine into a microparticle can extend drug release, thus avoiding multiple injections of traditional ropivacaine.

In this research, we used PCL with same Mn and different architectures (1-PCL and 4-PCL) as carriers. Since the power of the ultrasonic processor was fixed, we just adjusted nonultrasonic-related parameters during the investigation. PCL dosage, Ropi dosage, PVA concentration, and O/W ratio were systematically investigated to obtain optimized microspheres (supporting material Figure S2). Laser scattering was used to determine the size and size distribution of microspheres. Using a combined strategy including size parameter D [4,3] and size distribution parameter Span (Span = [D90 – D10]/D50), optimal microsphere preparation conditions were determined (Table 2). For single-armed PCL particles, 1-PCL concentration was 5% (*w*/*v*), ropivacaine concentration was 2% (*w*/*v*), PVA concentration was 1% (*w*/*v*), and the O/W ratio was 1/10. For four-armed PCL particles, 4-PCL concentration was 3% (*w*/*v*), ropivacaine concentration was 1% (*w*/*v*), PVA concentration was 1% (*w*/*v*), and the O/W ratio was 1/10.

In the next experiments, similar weight of the two types of the microspheres was used. Since the DL and EE were similar for both microspheres, entrapped ropivacaine could be controlled by the weight of the microspheres.

To investigate whether Ropi was encapsulated into the PCL microsphere or blended on the PCL surface, FT-IR tests were conducted. The FT-IR spectra of the blank 1-PCL and 4-PCL did not show any significant differences (Figures 3(a) and 3(b)) because the dominant groups are the same in 1-PCL and 4-PCL. Ropi showed characteristic absorbances corresponding to the structure of ropivacaine

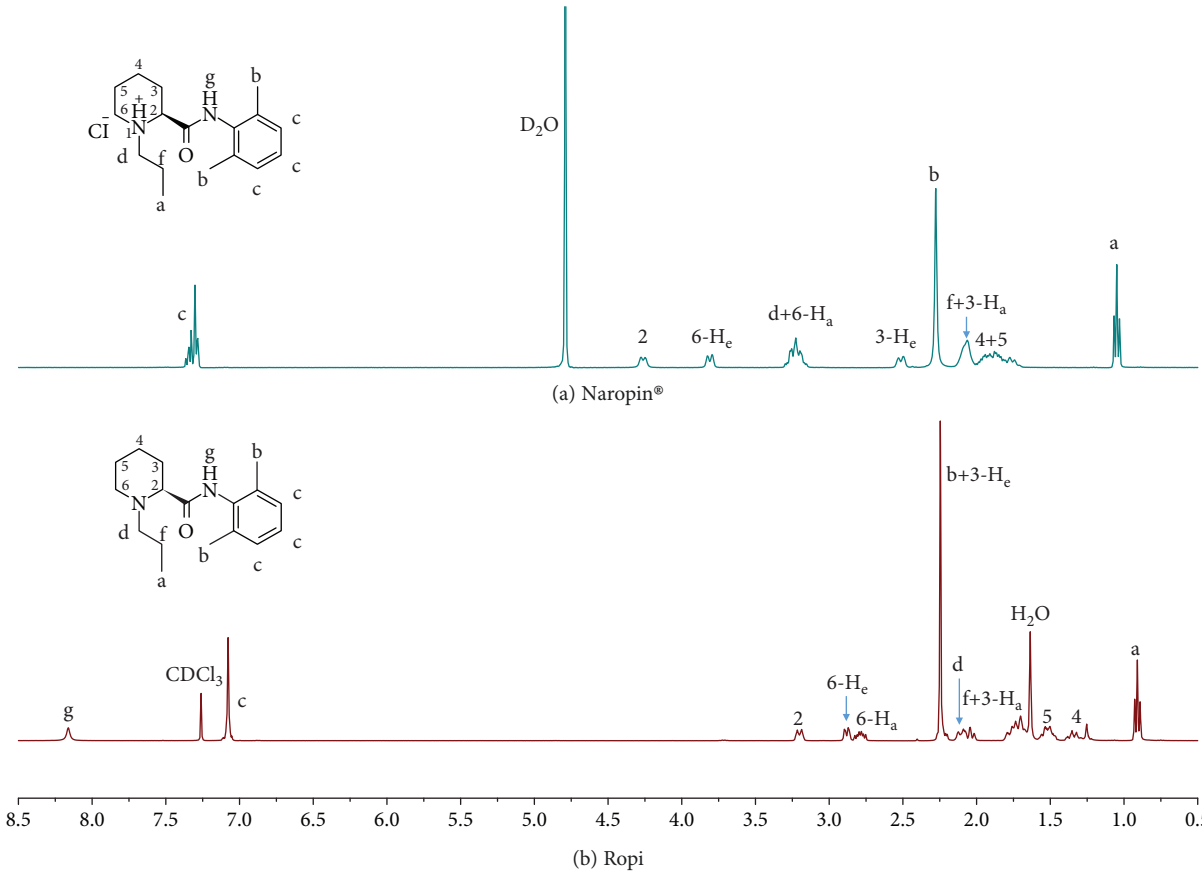

Figure 2: ^{1}H NMR spectra of Naropin® (a) and Ropi (b).

Table 2: Optimal preparation parameters of the microspheres.

Group[1]	[Ropi] (mg/mL)	[PCL] (mg/mL)	[PVA] (mg/mL)	O/W ratio	D[4,3] (μm)	Span	DL (%)	EE (%)
1	2	5	1	1/5	41.56	2.008	75.39%	22.64%
1a	1	3	1	1/8	73.31	3.737	70.51%	21.83%

[1]Group 1 used 1-PCL as a carrier. Group 1a used 4-PCL as a carrier.

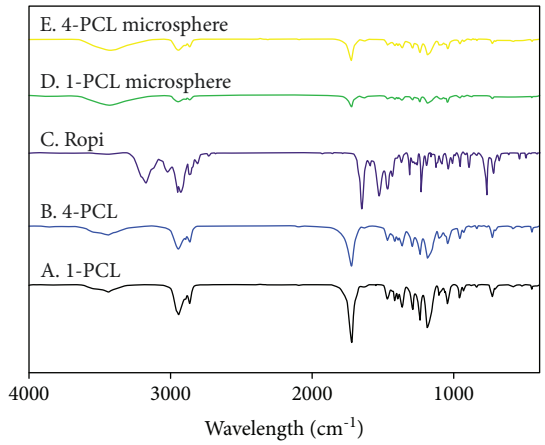

Figure 3: FT-IR spectra of blank 1-PCL (A), blank 4-PCL (B), Ropi (C), Ropi-loaded 1-PCL microsphere (D), and Ropi-loaded 4-PCL microsphere (E).

(Figure 3(c)). After drug loading, only PCL characteristic peaks appeared, while the peaks corresponding to Ropi could barely be seen (Figures 3(d) and 3(e)). This indicated that Ropi was basically encapsulated into the PCL microsphere other than being inserted on the PCL surface. Besides, Ropi did not react with PCL as the intensity of the characteristic IR peak decreased and no obvious peak movement occurred.

Both the blank microsphere and the drug-loading microsphere showed diffraction peaks corresponding to PCL at 20-25° (Figures 4(a) and 4(b)). XRD data confirmed the crystallinity of the blank single-armed PCL particle was 69.95% and 69.00% for 4-PCL (Figure 4(c)). The crystallinity of both PCL carriers was similar. Half-peak width of the 4-PCL diffraction peak was larger than that of the 1-PCL. The grain size formed by 4-PCL was smaller than that by 1-PCL. This may originate from shorter chains of 4-PCL compared to 1-PCL, which promotes the formation of

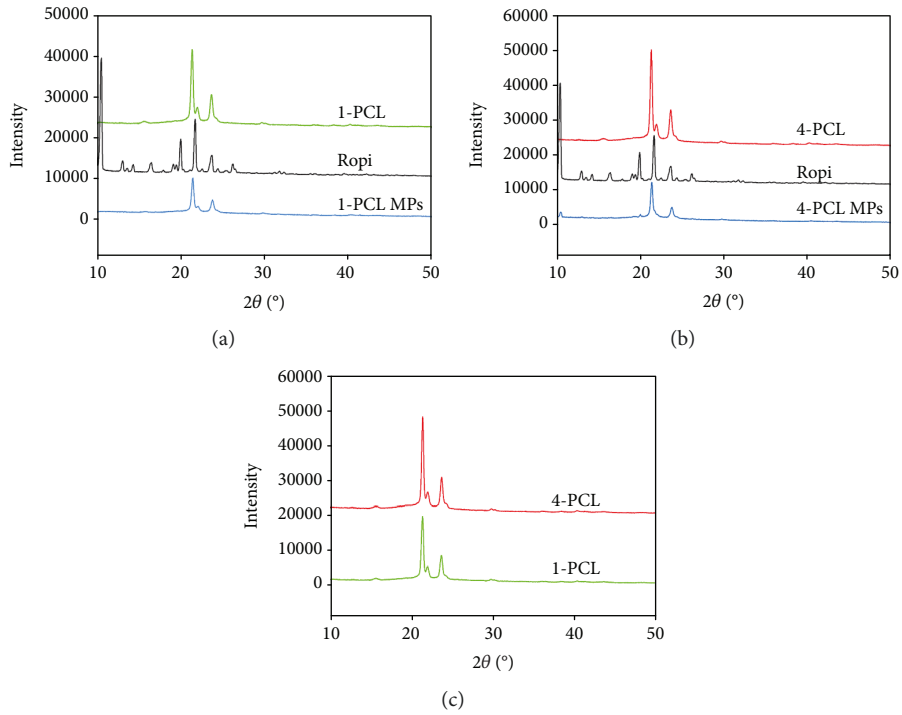

Figure 4: XRD spectra of the blank 1-PCL and the Ropi-loaded 1-PCL microsphere (a) and the blank 4-PCL and the Ropi-loaded 4-PCL microsphere (b) and comparison between the blank 1-PCL and the blank 4-PCL (c).

smaller grains. XRD also confirmed drug loading did not affect the crystallinity of 1-PCL and 4-PCL. Compared to Ropi-loaded 1-PCL particles, the characteristic peak of Ropi was visible in the XRD spectra of Ropi-loaded 4-PCL particles (Figure 4(b)). From the FT-IR spectra, it can be deduced that Ropi is located shallowly beneath the 4-PCL carrier. Neither were new diffraction peaks present nor did any shift of the diffraction peak occur compared to the blank particles. This implied that there was no strong interaction between Ropi and PCL and that the microsphere preparation process does not hinder the crystallization of PCL.

3.4. Ropivacaine Release In Vitro. We used the optimal particles to conduct an *in vitro* release assay to analyze different release behaviors of 1-PCL and 4-PCL particles. As shown in Figures 5(a) and 5(b), both Ropi-loaded 1-PCL and 4-PCL particles were smooth spheres. The size of optimal 4-PCL spheres was smaller than that of 1-PCL spheres due to the lower 4-PCL concentration used in particle preparation as shown in Table 2. It can be observed that there was an increase in the size of both 1-PCL and 4-PCL spheres after the release assay. Moreover, the spheres generally adhered to each other during the release progress, and all spheres still maintained their smooth shape even under severe adhesion (Figures 5(c) and 5(d)).

It is assumed that Ropi is generally released from the particles while PCL does not obviously degrade during this period. Ropi was released slowly from the 4-PCL sphere compared to the 1-PCL sphere in the first 8 h. This might originate from the obstruction of small 4-PCL grains. Both spheres were then adjusted to have similar Ropi release rates until they reached the maximum accumulated Ropi amount in 58 h. The higher the concentration of Ropi used during the preparation of 1-PCL spheres, the higher the amount of Ropi was observed during the *in vitro* release assay (Figure 6). Accumulated Ropi concentrations were 1766.4 μg and 1651.9 μg for 1-PCL and 4-PCL spheres, respectively.

3.5. Cytotoxicity of the Ropivacaine Microspheres. We used the release sample to assess the cytotoxicity of the ropivacaine microspheres. Cells cultured in wells without the addition of a release sample served as the control. The CCK-8 assay was applied to evaluate the cytotoxicity of the ropivacaine-loaded microspheres. L929 fibroblasts seeded on the 96-well plate proliferated well after the addition of the release sample (Figure 7). The O.D. value indicated that the release sample of the ropivacaine microspheres had no obvious toxicity. These results show that the ropivacaine microspheres are biocompatible.

4. Conclusion

We have carried out systematic studies towards the preparation of Ropi-loaded PCL particles. 1-arm PCL and 4-arm PCL with similar molecular weights and different architectures were prepared by ring-opening polymerization. High solubility of ropivacaine hydrochloride (Naropin®) does not favor particle preparation. Hence, we neutralized Naropin® to obtain pure ropivacaine (Ropi). We confirmed that the

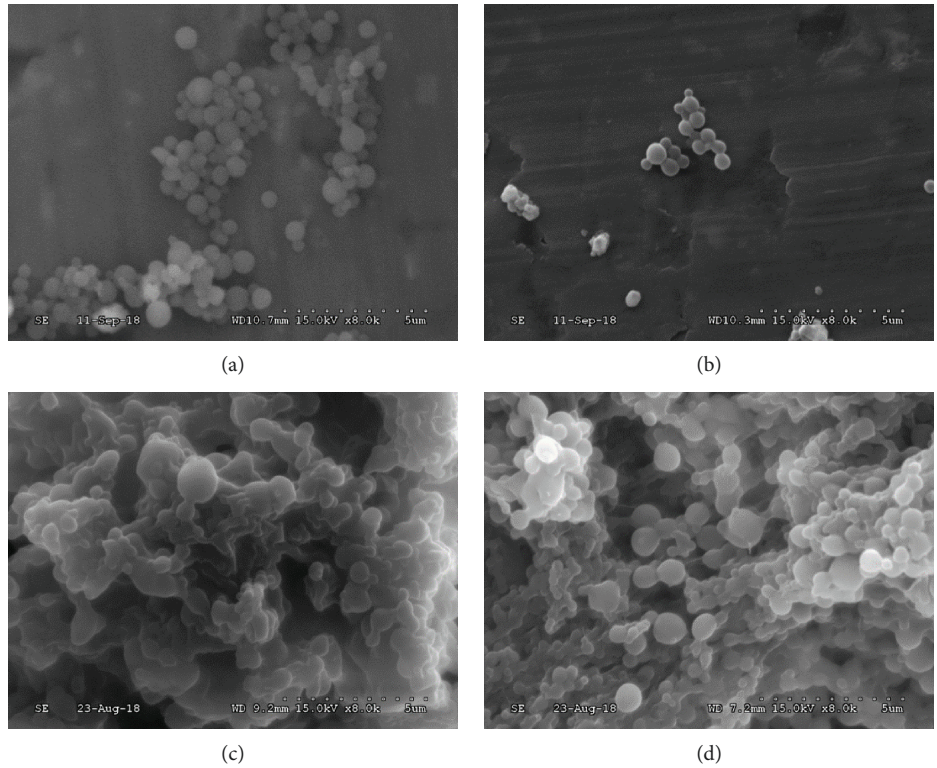

Figure 5: SEM images of Ropi-loaded 1-PCL spheres (a), Ropi-loaded 4-PCL spheres (b), 1-PCL spheres after release assay for 58 h (c), and 4-PCL spheres after release assay for 58 h (d). The scale bar = 5 μm.

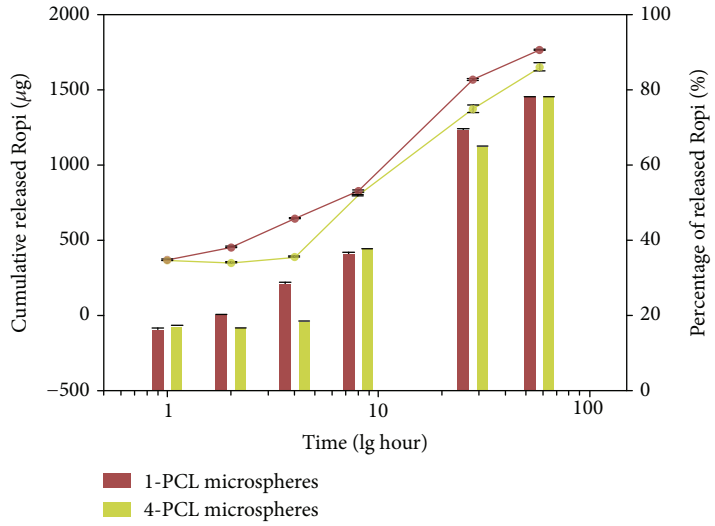

Figure 6: Accumulated Ropi released from 1-PCL spheres (red) and 4-PCL spheres (green). Ratio of released Ropi is displayed as the bar chart.

structure of ropivacaine was maintained during neutralization which did not alter the analgesia mechanism.

We made clarifications on the specific roles of each reagent during microsphere preparation. Evaluation of size, size distribution, drug loading, and encapsulated efficiency were conducted so as to determine the optimal PCL preparation conditions. Smooth microspheres were prepared under the optimized conditions. We confirmed Ropi was completely encapsulated by PCL. In addition, the encapsulation process does not interfere with the crystallinity of the PCL. *In vitro* release assay indicated 4-PCL hindered the release of Ropi during the first 8 h. However, the hindrance generally decays as the Ropi release rate tends to be similar during the consecutive assay. Both spheres reached maximum

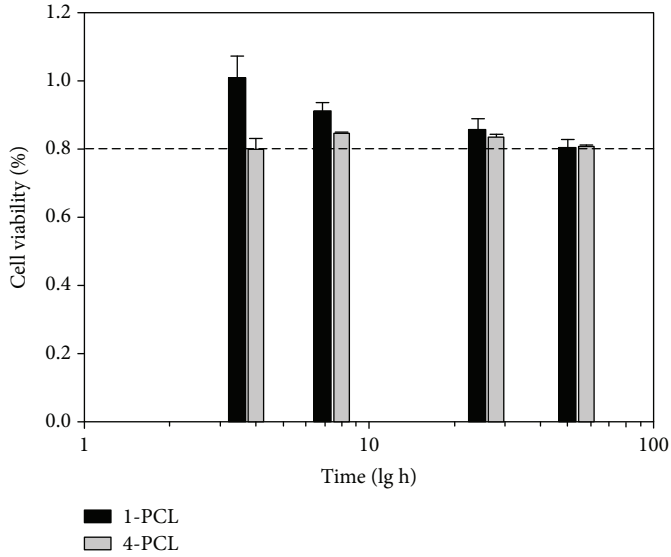

Figure 7: Cytotoxicity of ropivacaine-loaded PCL microspheres to L929 cells (CCK-8 test).

Ropi-accumulated concentration at 58 h. The cytotoxicity assay revealed PCL microspheres loaded with ropivacaine were biocompatible. Hence, our experiments confirm that the architecture of the PCL carrier does not significantly affect the release of ropivacaine and also that the incorporation of ropivacaine does not interfere with the biocompatibility of PCL.

Data Availability

The data used to support the findings of this study are available from the corresponding authors upon request.

Conflicts of Interest

The authors declared no potential conflicts of interest with respect to the research, authorship, and/or publication of this article.

Authors' Contributions

Wei Xiong and Yue-kun Shen contributed equally to the article.

Acknowledgments

Mouse fibroblast L929 cells were kindly provided by Prof. Dr. Daping Quan from the School of Chemistry of Sun Yat-sen University. This work was financially supported by the National Natural Science Foundation of China (No. 81571032).

Supplementary Materials

Generally, there are 2 parts included in the uploaded supplementary material. Supplementary Figure S1A showed the absorption curve of neutralized ropivacaine in dichloromethane. Based on the maximum absorption at each concentration, the standard working curve had been established in Figure S1B. To quantify ropivacaine released to PBS, the standard ropivacaine working curve in PBS also had been set up as shown in Figure S1C. In the second part, we investigated characters affecting morphology of microspheres during preparation. Dosage of ropivacaine, PCL, PVA, and ratio of oil phase to water phase (O/W ratio) were investigated. The results were listed in supplementary Table S1-S4. Drug loading (DL), encapsulation efficiency (EE), and morphological characters such as Span were recorded. To intuitively reflect the results indicated in Table S1-S4, supplementary Figure S2 was established. After evaluation of each characters, the optimal microsphere preparation condition was selected and presented in the main body of the article. *(Supplementary Materials)*

References

[1] K. Knudsen, M. Beckman Suurküla, S. Blomberg, J. Sjövall, and N. Edvardsson, "Central nervous and cardiovascular effects of i.v. infusions of ropivacaine, bupivacaine and placebo in volunteers," *British Journal of Anaesthesia*, vol. 78, no. 5, pp. 507–514, 1997.

[2] J. H. McClure, "Ropivacaine," *British Journal of Anaesthesia*, vol. 76, no. 2, pp. 300–307, 1996.

[3] G. R. Harrison, "The use of epidural ropivacaine in high doses for the management of pain from invasive carcinoma of the cervix," *Anaesthesia*, vol. 54, no. 5, pp. 459–461, 1999.

[4] L. Lemos, R. Fontes, S. Flores, P. Oliveira, and A. Almeida, "Effectiveness of the association between carbamazepine and peripheral analgesic block with ropivacaine for the treatment of trigeminal neuralgia," *Journal of Pain Research*, vol. 3, pp. 201–212, 2010.

[5] J. H. Rosland and J. T. Geitung, "CT guided neurolytic blockade of the coeliac plexus in patients with advanced and intractably painful pancreatic cancer," *Scandinavian Journal of Pain*, vol. 18, no. 2, pp. 247–251, 2018.

[6] K. J. McClellan and D. Faulds, "Ropivacaine," *Drugs*, vol. 60, no. 5, pp. 1065–1093, 2000.

[7] C. B. Christiansen, M. H. Madsen, C. Rothe, A. M. Andreasen, L. H. Lundstrøm, and K. H. W. Lange, "Volume of ropivacaine 0.2% and common peroneal nerve block duration: a randomised, double-blind cohort trial in healthy volunteers," *Anaesthesia*, vol. 73, no. 11, pp. 1361–1367, 2018.

[8] A. K. Abdulall, M. M. Tawfick, A. R. El Manakhly, and A. El Kholy, "Carbapenem-resistant Gram-negative bacteria associated with catheter-related bloodstream infections in three intensive care units in Egypt," *European Journal of Clinical Microbiology & Infectious Diseases*, vol. 37, no. 9, pp. 1647–1652, 2018.

[9] A. Mushtaq, B. Navalkele, M. Kaur et al., "Comparison of complications in midlines versus central venous catheters: Are midlines safer than central venous lines?," *American Journal of Infection Control*, vol. 46, no. 7, pp. 788–792, 2018.

[10] W. Zhang, W. Xu, C. Ning et al., "Long-acting hydrogel/microsphere composite sequentially releases dexmedetomidine and bupivacaine for prolonged synergistic analgesia," *Biomaterials*, vol. 181, pp. 378–391, 2018.

[11] W. Zhang, C. Ning, W. Xu et al., "Precision-guided long-acting analgesia by hydrogel-immobilized bupivacaine-loaded microsphere," *Theranostics*, vol. 8, no. 12, pp. 3331–3347, 2018.

[12] Y. Zhang, T. Shams, A. H. Harker, M. Parhizkar, and M. Edirisinghe, "Effect of copolymer composition on particle morphology and release behavior *in vitro* using progesterone," *Materials & Design*, vol. 159, pp. 57–67, 2018.

[13] J. Rodríguez Villanueva and L. Rodríguez Villanueva, "Turning the screw even further to increase microparticle retention and ocular bioavailability of associated drugs: The bioadhesion goal," *International Journal of Pharmaceutics*, vol. 531, no. 1, pp. 167–178, 2017.

[14] W. Chen, Q. Ni, L. Tong, J. Cao, and C. Ji, "Preparation of novel biodegradable ropivacaine microspheres and evaluation of their efficacy in sciatic nerve block in mice," *Drug Design, Development and Therapy*, vol. Volume 10, pp. 2499–2506, 2016.

[15] H. Tian, Z. Chen, Y. Liu, and L. Liu, "The sustained-release of ropivacaine PLGA microspheres in the mouse sciatic nerve," *Chinese Journal of Pain Medicine*, vol. 16, no. 05, pp. 296–299, 2010.

[16] Y. Zhai, X. Yang, L. Zhao, Z. Wang, and G. Zhai, "Lipid nanocapsules for transdermal delivery of ropivacaine: in vitro and *in vivo* evaluation," *International Journal of Pharmaceutics*, vol. 471, no. 1–2, pp. 103–111, 2014.

[17] J. B. Jonnalagadda, I. V. Rivero, and J. Warzywoda, "In-vitro degradation characteristics of poly(e-caprolactone)/poly(glycolic acid) scaffolds fabricated via solid-state cryomilling," *Journal of Biomaterials Applications*, vol. 30, no. 4, pp. 472–483, 2015.

[18] N. Qiang, W. Yang, L. Li et al., "Synthesis of pendent carboxyl-containing poly(ε-caprolactone-co-β-malic acid)-block-poly(*l*-lactide) copolymers for fabrication of nanofibrous scaffolds," *Polymer*, vol. 53, no. 22, pp. 4993–5001, 2012.

[19] Y. Zhang, S. Luo, Y. Liang et al., "Synthesis, characterization, and property of biodegradable PEG-PCL-PLA terpolymers with miktoarm star and triblock architectures as drug carriers," *Journal of Biomaterials Applications*, vol. 32, no. 8, pp. 1139–1152, 2018.

[20] A. C. Vieira, J. C. Vieira, J. M. Ferra, F. D. Magalhães, R. M. Guedes, and A. T. Marques, "Mechanical study of PLA–PCL fibers during in vitro degradation," *Journal of the Mechanical Behavior of Biomedical Materials*, vol. 4, no. 3, pp. 451–460, 2011.

[21] N. Qiang, S. Tang, X. J. Shi et al., "Synthesis of functional polyester for fabrication of nano-fibrous scaffolds and its effect on PC12 cells," *Journal of Biomaterials Science. Polymer Edition*, vol. 27, no. 3, pp. 191–201, 2016.

[22] Y. Zhang, Y. Yue, and M. Chang, "Local anaesthetic pain relief therapy: *In vitro* and *in vivo* evaluation of a nanotechnological formulation co-loaded with ropivacaine and dexamethasone," *Biomedicine & Pharmacotherapy*, vol. 96, no. 89, pp. 443–449, 2017.